MULTISCALE DIRECTIONAL AM-FM DEMODULATION OF IMAGES USING A 2D OPTIMIZED METHOD

Victor Murray[*], *Marios S. Pattichis*[*], *and Peter Soliz*[♮]

[*]University of New Mexico, Department of Elect. and Comp. Eng., Albuquerque, New Mexico, USA.
[♮]VisionQuest Biomedical, Albuquerque, New Mexico, USA.
E-mails: vmurray@ieee.org, pattichis@ece.unm.edu, psoliz@visionquest-bio.com

DRAFT

ABSTRACT

We present an improved and optimized formulation for the estimation of the multiscale amplitude-modulation frequency-modulation (AM-FM) estimates when (i) non-separable filters are used and (ii) the variable spacing, local linear phase method is used. Also, we introduce the use of multiscale directional filterbanks for the feature extraction of images.

Recently, AM-FM methods have shown promising results in a variety of medical image analysis applications. The 2D optimized AM-FM demodulation described here presents advantages for feature extraction at different frequency scales and orientations that can be used to detect different patterns, directions, or structures in an image.

We test the new formulation using a Gaussian amplitude-modulated Quadratic frequency-modulated synthetic image and natural images. The results show that the optimized estimation produces better results, up to 4.9 times for the IF estimation and in 3 orders of magnitude for the IA estimation, for noise-free signals compared to the state-of-the-art methods.

***Index Terms*—** amplitude-modulation frequency-modulation (AM-FM), multi-scale analysis

1. INTRODUCTION

We consider the AM-FM demodulation based on a variable spacing, local linear phase (VS-LLP) method presented in [1,2] and applied in applications such as [3–5]. The VS-LLP method belongs to the AM-FM demodulation methods based on the notion of a Hilbert-based extension of the 1-D Hilbert-based demodulation approach. Early work can be found in Havlicek's dissertation [6]. The phase quadrature transform for extending the Hilbert transform into two dimensions was introduced in [7, 8]. Then, Felsberg and Sommer introduced the monogenic signal, an extension of the analytic signal to images in [9]. Note that, as discussed by Havlicek in [6], the proposed approach satisfies 3 conditions: (i) amplitude continuity and differentiability, (ii) phase independence of scaling and homogeneity, and (iii) harmonic correspondence.

Recently, significant applications in many areas of image processing, specially for medical imaging, have been using amplitude-modulation frequency-modulation (AM-FM) image decompositions. Thus, the development of more accurate AM-FM methods is required. AM-FM applications range from electron microscopy image segmentation and classification in [10], breast cancer images [11], optical coherence tomography [12,13], carotid artery [4], magnetic resonance imaging [3], pneumoconiosis [14] to diabetic retinopathy [5], and age-related macula degeneration [15]. These applications use the advantages of the AM-FM demodulation methods in terms of the features extraction to detect different patterns, directions, or structures in an image.

The use of multiscale directional filterbanks for the feature extraction of images when orientation matters will provide extra information the medical applications described in the previous lines. Nguyen presented some analysis in [16,17] that can be related with the use of directions. Here, our focus is in the development of multiscale directional AM-FM methods.

In the rest of the document, we describe the methodology used for the improved and optimized 2D formulation for the AM-FM estimation when non-separable filters are used. In Section 2, we present the proposed methodology. Results and a discussion are given in Section 3. Finally, conclusions are presented in Section 4.

2. METHODOLOGY

2.1. AM-FM demodulation method in medical applications

We consider a multi-scale AM-FM representation of digital non-stationary images given by [1,2]

$$I(k_1,k_2) \simeq \sum_{n=1}^{M} a_n(k_1,k_2)\cos\varphi_n(k_1,k_2), \qquad (1)$$

where $n = 1,2,\ldots,M$ denote different frequency scales, a_n denotes the instantaneous amplitude (IA) functions, and φ_n denotes the instantaneous phase (IP) functions. We define each scale in terms of a collection of bandpass filters that share similar frequency magnitude ranges. As an example, in Fig. 1a, we have *low* (filters 14-19), *medium* (filters 8-13), and *high* (filters 2-7) frequency scales. We only consider scales derived from a dyadic filterbank decomposition described in [1,5]. The IA functions are assumed to be slowly varying over the image. High values of the IA signify strong presence of the corresponding combination of scales. Texture variations are captured by the FM functions $\cos\varphi$. Associated with each AM-FM component, we have the instantaneous frequency (IF) $\nabla\varphi = (\varphi_x, \varphi_y)$.

The input images are first filtered through an extended 2-D Hilbert filter. The output is then processed through a dyadic filterbank. Current applications (see for example [1,3–5]) use separable filters grouped by frequency scales (see Fig. 1a). Then, the AM-FM demodulation is applied at the output of each bandpass filter. At each pixel, the AM-FM estimate with the largest value of the IA is selected. Thus, the approach is to basically to apply *dominant*

This work was supported in part by the National Eye Institute under Grants EY018280 and EY020015.

component analysis (DCA) within each group of filters (see [6] for DCA).

The AM-FM demodulation algorithm is summarized as: using the output of each bandpass filter, we estimate the IA and IP using: $\hat{a}(k_1,k_2) = |\hat{I}_{AS}(k_1,k_2)|$ and $\hat{\varphi}(k_1,k_2) = \arctan(\text{imag}(\hat{I}_{AS}(k_1,k_2))/\,\text{real}(\hat{I}_{AS}(k_1,k_2))$, respectively, with $\hat{I}_{AS}(k_1,k_2) = I(k_1,k_2) + j\mathcal{H}_{2d}[I(k_1,k_2)]$, where $\mathcal{H}_{2d}$ denotes a two-dimensional extension of the one-dimensional Hilbert transform operator. For robust IA and IF estimations, a variable spacing, local linear phase (VS-LLP) method, as described in [1,2], is used. Here, for estimating the first component, we generate four estimates using

$$\hat{\varphi}_x(k_1,k_2) = \frac{1}{n_1}\arccos\left(\gamma\left(n_1\right)\right), \tag{2}$$

where $\bar{I}_{AS}(k_1,k_2) = \hat{I}_{AS}(k_1,k_2)/|\hat{I}_{AS}(k_1,k_2)|$ and $\gamma\left(n_1\right) = \left(\bar{I}_{AS}(k_1+n_1,k_2) + \bar{I}_{AS}(k_1-n_1,k_2)\right) / \left(2\bar{I}_{AS}(k_1,k_2)\right)$. For the second component direction $\hat{\varphi}_2$ we perform a similar approach.

According to [1,2], n_1 represents a variable displacement, from 1 to 4 formulated from the optimization problem

$$\begin{aligned} &\underset{n_1}{\text{minimize}} \quad |\gamma_{\arccos}(n_1)| \\ &\text{subject to} \quad \hat{\varphi}_x \in [w_{p_{1x}}, w_{p_{2x}}], \end{aligned} \tag{3}$$

where $w_{p_{1x}}$ and $w_{p_{2x}}$ represents the cut-off frequencies of the bandpass used projected to the x-direction. For example, for the bandpass labeled as 13 in Fig. 1a, $[w_{p_{1x}}, w_{p_{2x}}] = [\pi/4,\ \pi/2]$.

2.2. Proposed AM-FM estimation for non-separable filters

The method described in subsection 2.1 is producing good results in many applications such as [3–5,14]. However, when a non-separable filterbank is used, the optimization from (3) cannot be solved independently for $\hat{\varphi}_x$ and $\hat{\varphi}_y$.

Let's consider the filterbank shown in Fig. 1b. This filterbank follows the idea of the fan and directional filters described in [18]. For the 2D problem, let's analyze only 1 filter as shown in Fig. 1c. The region labeled as $\mathcal{A}$ indicates the support of the bandpass filter within a range of instantaneous frequencies $(\hat{\varphi}_x, \hat{\varphi}_y)$ for both directions at the same time.

For the variable spacing optimization used by the VS-LLP method we analyze both x and y directions at the same time. We consider

$$\begin{aligned} &\underset{n_1,n_2}{\text{minimize}} \quad (|\gamma_{\arccos}(n_1)| + |\gamma_{\arccos}(n_2)|) \\ &\text{subject to} \quad (\hat{\varphi}_x, \hat{\varphi}_y) \in \mathcal{A}, \end{aligned} \tag{4}$$

where $\gamma\left(n_1\right)$ was defined in the previos subsection, $\gamma\left(n_2\right) = \left(\bar{I}_{AS}(k_1,k_2+n_2) + \bar{I}_{AS}(k_1,k_2-n_2)\right) / \left(2\bar{I}_{AS}(k_1,k_2)\right)$, and $\mathcal{A}$ is considered to be the region of the bandpass filter. In this case (see Fig. 1c), the region $\mathcal{A}$ is composed by the frequencies with angle $\theta \in [\xi - \triangle\xi, \xi + \triangle\xi]$ and with radius $\rho \in [w_{p_1}, w_{p_2}]$. Note that $\gamma\left(n_1\right)$ and $\gamma\left(n_2\right)$ are the argument of the trigonometric functions for computing $(\hat{\varphi}_x, \hat{\varphi}_y)$ (see (2)).

2.3. Multiscale Directional Filterbank

We use a multiscale directional filterbank implementation similar to Figs. 1b-c. The filters are generated in two steps: (i) we implement the circular filters first and then, (ii) we implement the directional filters.

First, based on the optimized 1D filter design (see [1,2]), we produce 2D filters using a frequency transformation from 1D to 2D

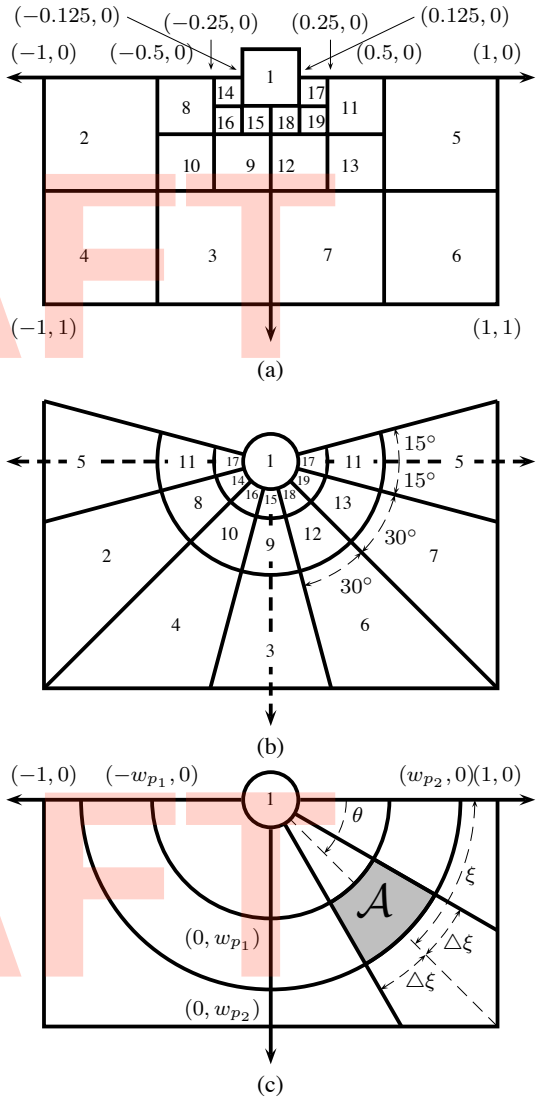

Fig. 1. Filterbanks used for the AM-FM applications. We show the 2D frequency spectrum in normalized frequencies. (a) Current dyadic multiscale filterbank (3-scale) used in [1,3–5]. The design is based in separable 1D filters. (b) Multiscale directional filterbank based on non-separable filters. The cut-off frequencies in x and y are similar to (a). In this example, each filter has an angular extension of 30°. (c) Example for the analysis of one bandpass filter with a coverage of the x and y frequencies in the region $\mathcal{A}$.

based on [19]. The cut-off frequencies are given by $w_{p_1} \leq \rho \leq w_{p_2}$ (see Fig. 1c) in terms of polar coordinates (ρ, θ) such that $(u, v) = (\rho\cos\theta, \rho\sin\theta)$, where (u, v) are the frequency cartesian coordinates of (k_1, k_2),

Then, in terms of the directional filters, one solution is to use the methods created in [20,21]. However, for flexibility in the implementation (see Figs. 1b-c), we use a simple method for producing directional filters based on a frequency design. Given a desired orientation ξ with a spread of $\pm\triangle\xi$ (the filter covers the angles θ from $\xi - \triangle\xi$ to $\xi + \triangle\xi$, see Fig. 1c), with a transition band of $\delta\xi$, we

DRAFT

generate a frequency mask $M_p(\rho,\theta)$ such that (in polar coordinates):

$$M_p(\rho,\theta)=\begin{cases}1, & \xi-\triangle\xi\le\theta\le\xi+\triangle\xi,\\ 0, & \theta<\xi-\triangle\xi-\delta\xi,\\ 0, & \theta>\xi+\triangle\xi+\delta\xi,\\ \frac{\theta-(\xi-\triangle\xi-\delta\xi)}{\delta\xi}, & \xi-\triangle\xi-\delta\xi\le\theta<\xi-\triangle\xi,\\ \frac{\xi+\triangle\xi+\delta\xi-\theta}{\delta\xi}, & \xi+\triangle\xi<\theta\le\xi+\triangle\xi+\delta\xi.\end{cases}$$

This function produces a linear change from 0 to 1 in the transition bands defined by $\delta\xi$. To reduce the ringing problem in the design, we apply a 3×3 Gaussian filter $G(u,v)$ to the mask: $M(u,v)=M_p(u,v)*G(u,v)$ (where $M_p(u,v)$ is $M_p(\rho,\theta)$ in cartesian coordinates). Then, the directional filter in space domain is defined as $h_{directional}(x,y)=\Im^{-1}\{M(u,v)\}$, where $\Im^{-1}\{\cdot\}$ is the 2D inverse Fourier transform.

3. RESULTS AND DISCUSSION

3.1. Parameters used in the filterbank

We use both a 2-scale and a 3-scale filterbank designed based on Figs. 1b-c. The orientations for the directional filterbanks are $\xi=0,30,60,90,120,150^\circ$ with an expansion of $\triangle\xi=20^\circ$ and a transition band of $\delta\xi=10,20^\circ$.

The circular frequency scales follow the cut-off frequencies shown in Fig. 1a: $[0,\pi/4,\pi/2,\pi]$ and $[0,\pi/8,\pi/4,\pi/2,\pi]$ for a 2-scale and a 3-scale filterbank, respectively.

3.2. Images used

To test the accuracy of the proposed method, we use the Gaussian amplitude-modulated Quadratic frequency-modulated synthetic image used in [1]. This signal is defined as: $I(k_1,k_2)=100\exp\left[-\frac{1}{2}\alpha^2\left(\left(\frac{k_1+\frac{1}{2}}{\frac{N}{2}}\right)^2+\left(\frac{k_2+\frac{1}{2}}{\frac{N}{2}}\right)^2\right)\right]\cos\varphi(k_1,k_2)$, for $k_1,k_2=-\frac{N}{2},\ldots,\frac{N}{2}-1$, $\alpha=2.5$ and $N=1024$. The phase with $\varphi_x(k_1,k_2)\in[\pi/6,\pi/5]$ and $\varphi_y(k_1,k_2)=-\varphi_x(k_1,k_2)$.

Also, we use a natural image of a *zebra* (see Fig. 2a) to show the potential use of the directional analysis using AM-FM methods. We picked up a *zebra* due to the nice multiscale directional structures that it has in its stripes.

3.3. Multiscale Directional AM-FM demodulation

We compare the results of the proposed method with the results shown in [1] for the noise-free synthetic signal described before. In Table 1 we show the mean-squared-error (MSE) results for the IA and IF in the x-direction (the results for y are similar) using the filterbanks described in subsection 3.1.

In Fig. 2, we present the analysis of the AM-FM demodulation of the *zebra* using a 3-scale filterbank with $\delta\xi=10$. We show the FM results using the lowpass filter (LPF, filter 1 in Fig. 1b) in Fig. 2b and using the low-high frequencies in Figs. 2c-h in orientations at 0°, 30°, 60°, 90°, 120°, and 150°. The FM images have been thresholded using the mean of the IA (high IA values).

3.4. Discussion

We can see from Table 1 that the proposed method produced better results than those currently used as state-of-the-art such as [1, 22]. The use of more scales (3-scales compared to 2-scales) always implies more accurate estimations. This effect is observed for both the IA and the IF estimations, for any method: the proposed 2D optimized VS-LLP, the quasi-eigenfunction approximation (QEA) method from [22], and the VS-LLP from [1].

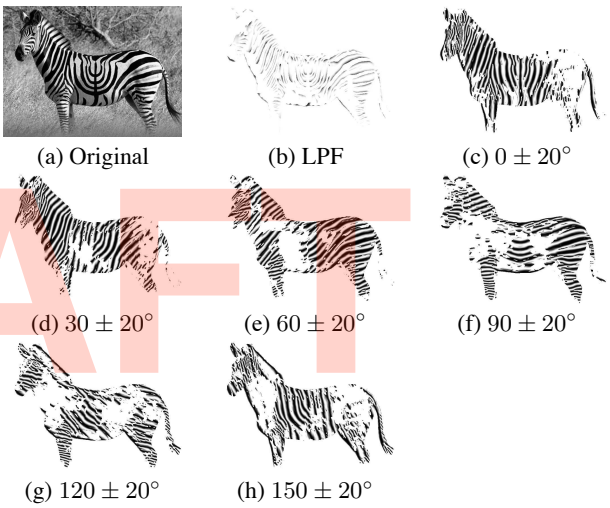

(a) Original (b) LPF (c) $0\pm 20^\circ$ (d) $30\pm 20^\circ$ (e) $60\pm 20^\circ$ (f) $90\pm 20^\circ$ (g) $120\pm 20^\circ$ (h) $150\pm 20^\circ$

Fig. 2. Analysis of the image *zebra* using a 3-scale filterbank with 6 directions. (a) Original image. (b) FM of (a) thresholded at the mean of IA using the lowpass filter (LPF). (c), (d), (e), (f), (g), (h) FM of (a) thresholded at the mean of IA in the low to high frequencies (no LPF used) in the orientations at 0°, 30°, 60°, 90°, 120°, and 150°, respectively. The background of the *zebra* in (a) was manually removed for (b)-(h).

One important factor is the bigger the transition band of $\delta\xi$, the better the results. Also, note that we are using a bigger overlapping of the bandpass filters in terms of the directions. Each directional filter is oriented at $\xi\pm 20^\circ$ with $\xi=0,30,60,90,120,150^\circ$. This implies that for 2 continuous directions, for example $\xi=0^\circ$ and $\xi=30^\circ$, the direction for $\xi=0^\circ$ covers the angle range $[-20^\circ,20^\circ]$ and the direction for $\xi=30^\circ$ covers $[10^\circ,50^\circ]$. Thus, there is an overlapping of 10° for each continuous direction (we are considering only the passband frequencies and not the transition band $\delta\xi$). We can assume here that the filterbank used for the circular frequency scales with the cut-off frequencies shown in Fig. 1a (see [1,5]) with almost not overlapping could be improved to find an optimum value of frequency overlapping.

The IF results of the proposed method are in the range of $[1.6,4.9]$ times better than QEA and $[1.3,3.8]$ better than the non-2D-optimized VS-LLP method from [1]. The IA results were improved in 3 order of magnitude compared to the other methods. Here both QEA and VS-LLP from [1] produced the same results. Note that we have used the separable filterbanks (see Fig. 1a) for the QEA and VS-LLP results reported in [1].

When we applied the multiscale directional AM-FM analysis to a natural image of a *zebra* (see Fig. 2a) the results are promising. First, we can see in Fig. 2b that the AM-FM estimation in the LPF of the 3-scale filterbank produces a description of the very low information of the stripes in all directions in the FM. Then, when we do the analysis without the LPF (low, medium and high frequencies together) and using independent directions, we can see how for each directional filter (remember that each direction covers $\pm 20^\circ$) different structures of the stripes are selected. This approach can be used for applications were direction matters or for decomposition of image information by both orientations and scales at the same time.

DRAFT

Table 1. Results in terms of the MSE for the IA and the IF estimations for the Gaussian amplitude-modulated Quadratic frequency-modulated synthetic image described in subsection 3.2. We compare the results from the proposed method (columns 6-9) versus the results published in [1] for the VS-LLP method and the QEA. 2-s and 3-s are 2-scale and 3-scale filterbank, respectively. $\delta\xi$ is the transition band used in the directional filter.

	2-s QEA	3-s QEA	2-s from [1]	3-s from [1]	2-s, $\delta\xi = 10$	2-s, $\delta\xi = 20$	3-s, $\delta\xi = 10$	3-s, $\delta\xi = 20$
IA	0.035	0.033	0.035	0.033	0.890×10^{-4}	0.812×10^{-4}	0.23×10^{-4}	0.20×10^{-4}
IF	2.34×10^{-8}	1.45×10^{-8}	2.45×10^{-8}	1.11×10^{-8}	1.257×10^{-8}	1.036×10^{-8}	0.885×10^{-8}	0.294×10^{-8}

4. CONCLUSIONS

We have developed a new, 2D optimized formulation for AM-FM estimations to be applied with non-separable filters. We have also introduced the analysis of the AM-FM estimates computed by different frequency scales and by different directions.

The results are improved up to 4.9 times for the IF estimation and in 3 orders of magnitude for the IA estimation for the Gaussian amplitude-modulated Quadratic frequency-modulated synthetic image used.

The proposed method shows promising results for the analysis of images rich in multiscale and directional structures.

The new multiscale directional design presents two major advantages: (i) the filters capture not only the spatial, but also the directionality of an image structure, (ii) one of the features used is the IF magnitude, for a fixed scale, using the filterbank from Fig. 1a, we dont have a constant range but with the new design, the range will be constant from w_{p_1} to w_{p_2}.

5. REFERENCES

[1] V. Murray, P. Rodriguez, and M. Pattichis, "Multi-scale AM-FM demodulation and image reconstruction methods with improved accuracy," *IEEE Transactions on Image Processing*, vol. 19, no. 5, pp. 1138 –1152, May 2010.

[2] Victor Manuel Murray Herrera, *AM-FM Methods for Image and Video Processing*, Ph.D. thesis, University of New Mexico, 2008.

[3] C. Loizou, V. Murray, M. S. Pattichis, I. Seimenis, M. Pantziaris, and C. S. Pattichis, "Multi-scale amplitude modulation-frequency modulation (AM-FM) texture analysis of multiple sclerosis in brain MRI images," *to appear in IEEE Transactions on Information Technology in Biomedicine*, 2010.

[4] C. Loizou, V. Murray, M. Pattichis, M. Pantziaris, and C. Pattichis, "Multi-scale amplitude modulation-frequency modulation (AM-FM) texture analysis of ultrasound images of the intima and media layers of the carotid artery," *to appear in IEEE Transactions on Information Technology in Biomedicine*, 2010.

[5] C. Agurto, V. Murray, E. Barriga, S. Murillo, M. Pattichis, H. Davis, S. Russell, M. Abramoff, and P. Soliz, "Multiscale AM-FM methods for diabetic retinopathy lesion detection," *IEEE Transactions on Medical Imaging*, vol. 29, no. 2, pp. 502 –512, feb. 2010.

[6] J. P. Havlicek, *AM-FM Image Models*, Ph.D. thesis, The University of Texas at Austin, 1996.

[7] K.G. Larkin, D.J. Bone, and M.A. Oldfield, "Natural demodulation of two-dimensional fringe patterns. I. General background of the spiral phase quadrature transform," *Journal of the Optical Society of America A: Optics, Image Science, and Vision*, vol. 18, no. 8, pp. 1862–1870, August 2001.

[8] K.G. Larkin, "Natural demodulation of two-dimensional fringe patterns. II. Stationary phase analysis of the spiral phase quadrature transform," *Journal of the Optical Society of America A: Optics, Image Science, and Vision*, vol. 18, no. 8, pp. 1871–1881, August 2001.

[9] M. Felsberg and G. Sommer, "The Monogenic Signal," *IEEE Transactions on Signal Processing*, vol. 49, no. 12, pp. 3136–3144, December 2001.

[10] M.S. Pattichis, C.S. Pattichis, M. Avraam, A. Bovik, and K. Kyriacou, "AM-FM texture segmentation in electron microscopic muscle imaging," *IEEE Transactions on Medical Imaging*, vol. 19, no. 12, pp. 1253–1257, Dec. 2000.

[11] M. Y. Elshinawy, Jianchao Zeng, S.-C. B. Lo, and M. F. Chouikha, "Breast cancer detection in mammogram with AM-FM modeling and gabor filtering," in *Proc. 7th International Conference on Signal Processing*, Aug. 31–Sept. 4, 2004, vol. 3, pp. 2564–2567.

[12] A. Kartakoulis, E. Bousi, and C. Pitris, "AM-FM analysis of optical coherence tomography signals," in *Optical Coherence Tomography and Coherence Domain Optical Methods in Biomedicine XIII*, J.G. Fujimoto, J.A. Izatt, and V.V. Tuchin, Eds. 2009, vol. 7168, p. 71681M, SPIE.

[13] A. Kartakoullis, E. Bousi, and C. Pitris, "AM-FM techniques in optical coherence tomography," in *Optical Coherence Tomography and Coherence Techniques IV*, P.E. Andersen and B.E. Bouma, Eds. 2009, vol. 7372, p. 73720U, SPIE.

[14] V. Murray, M. Pattichis, and P. Soliz, "Retrieval and classification of pneumoconiosis chest radiograph images using multiscale AM-FM methods," in *Asilomar Conference on Signals, Systems and Computers*, November 2009.

[15] E.S. Barriga, V. Murray, C. Agurto, M.S. Pattichis, S. Russell, M.D. Abramoff, H. Davis, and P. Soliz, "Multi-scale AM-FM for lesion phenotyping on age-related macular degeneration," in *IEEE International Symposium on Computer-Based Medical Systems*, August 2009, pp. 1 –5.

[16] C.T. Nguyen and J.P. Havlicek, "Modulation domain texture decomposition," in *IEEE International Conference on Image Processing*, September 2010, pp. 2741 –2744.

[17] C.T. Nguyen and J.P. Havlicek, "Coherent texture decomposition using AM-FM model," in *IEEE Southwest Symposium on Image Analysis Interpretation*, May 2010, pp. 81 –84.

[18] L. Li, W. Qian, and L.P. Clarke, "X-ray medical image processing using directional wavelet transform," in *IEEE International Conference on Acoustics, Speech, and Signal Processing*, may 1996, vol. 4, pp. 2251 –2254 vol. 4.

[19] J.S. Lim, *Two-Dimensional Signal and Image Processing*, Prentice Hall PTR, September 1989.

[20] A.L. da Cunha, J. Zhou, and M.N. Do, "The nonsubsampled contourlet transform: Theory, design, and applications," *IEEE Transactions on Image Processing*, vol. 15, no. 10, pp. 3089 –3101, October 2006.

[21] R.H. Bamberger and M.J.T. Smith, "A filter bank for the directional decomposition of images: theory and design," *IEEE Transactions on Signal Processing*, vol. 40, no. 4, pp. 882 –893, Apr. 1992.

[22] J.P. Havlicek, D.S. Harding, and A.C. Bovik, "Multidimensional Quasi-Eigenfunction Approximations and multicomponent AM-FM models," *IEEE Transactions on Image Processing*, vol. 9, no. 2, pp. 227–242, February 2000.

DRAFT